This article was downloaded by: [Chongqing University]
On: 15 February 2014, At: 04:52
Publisher: Taylor & Francis
Informa Ltd Registered in England and Wales Registered Number: 1072954 Registered office: Mortimer House, 37-41 Mortimer Street, London W1T 3JH, UK

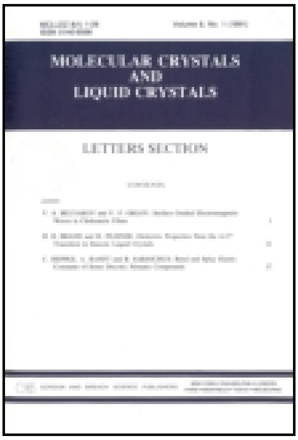

Molecular Crystals and Liquid Crystals
Publication details, including instructions for authors and subscription information:
http://www.tandfonline.com/loi/gmcl20

Enhanced Performance of Dye-Sensitized Solar Cells with Surface-Modified ZnO Nanorods

Seok Cheol Choi [a] , Won Suk Yun [a] & Sang Ho Sohn [a]
[a] Department of Physics , Kyungpook National University , Daegu , 702-701 , Korea

Published online: 08 Jan 2014.

To cite this article: Seok Cheol Choi , Won Suk Yun & Sang Ho Sohn (2013) Enhanced Performance of Dye-Sensitized Solar Cells with Surface-Modified ZnO Nanorods, Molecular Crystals and Liquid Crystals, 586:1, 88-94, DOI: 10.1080/15421406.2013.851536

To link to this article: http://dx.doi.org/10.1080/15421406.2013.851536

PLEASE SCROLL DOWN FOR ARTICLE

Taylor & Francis makes every effort to ensure the accuracy of all the information (the “Content”) contained in the publications on our platform. However, Taylor & Francis, our agents, and our licensors make no representations or warranties whatsoever as to the accuracy, completeness, or suitability for any purpose of the Content. Any opinions and views expressed in this publication are the opinions and views of the authors, and are not the views of or endorsed by Taylor & Francis. The accuracy of the Content should not be relied upon and should be independently verified with primary sources of information. Taylor and Francis shall not be liable for any losses, actions, claims, proceedings, demands, costs, expenses, damages, and other liabilities whatsoever or howsoever caused arising directly or indirectly in connection with, in relation to or arising out of the use of the Content.

This article may be used for research, teaching, and private study purposes. Any substantial or systematic reproduction, redistribution, reselling, loan, sub-licensing, systematic supply, or distribution in any form to anyone is expressly forbidden. Terms & Conditions of access and use can be found at http://www.tandfonline.com/page/terms-and-conditions

Mol. Cryst. Liq. Cryst., Vol. 586: pp. 88–94, 2013

ISSN: 1542-1406 print/1563-5287 online
DOI: 10.1080/15421406.2013.851536

Enhanced Performance of Dye-Sensitized Solar Cells with Surface-Modified ZnO Nanorods

SEOK CHEOL CHOI, WON SUK YUN, AND SANG HO SOHN*

Department of Physics, Kyungpook National University, Daegu 702-701, Korea

The surface destruction of the ZnO nanorod electrodes occurs in the dye-sensitization process, resulting in the extreme decreases of the short-circuit photocurrent density (J_{SC}), compared to TiO_2 electrodes. To solve these problems, the TiO_2 nanolayer is coated on the ZnO nanorod electrodes using a titanium tetrachloride ($TiCl_4$) assisted sonochemical process, which provides faster surface modification. The TiO_2 nanolayer can form new energy barrier on the ZnO nanorods, which can effectively inhibit the surface charge recombination and improve the energy conversion efficiency of the ZnO nanorod-based dye sensitized solar cells (DSSCs).

Keywords Dye-sensitized solar cell; sonochemical; surface modification; TiO_2 nanolayer; ZnO nanorod

Introduction

Dye-sensitized solar cells (DSSCs) provide a promising and cost-effective alternative to conventional solar cells because of their high power conversion efficiency, easy fabrication and low cost [1–3]. To date, much work has been performed on DSSCs fabricated with the different nanocrystalline oxide such as TiO_2, ZnO and SnO_2 to increase their electron transport characteristics. The investigation on ZnO nanorods as an alternative photoelectrode has been intensively carried out due to its band gap and conduction band edge energy which are nearly the same as TiO_2 [2]. Moreover, the electron mobility of ZnO is known to be 10^7 times larger than that of TiO_2 [4,5]. However, in the dye-sensitized process, the surface destruction of the ZnO nanorods occurs, resulting in an extreme decrease in photocurrent density (J_{SC}) [6]. A decrease in J_{SC} of ZnO-based DSSCs is attributable to more frequent recombination of photo-generated electrons in the conduction band with oxidized species in electrolytes [7]. In order to solve these problems, it needs the suppression of the recombination occurred in the ZnO electrode/dye and ZnO electrode/electrolyte interfaces.

In this work, we report the TiO_2 nanolayer coated on the ZnO nanorods as a new energy barrier using a $TiCl_4$ assisted sonochemical process, considering that they can effectively inhibit the recombination of and improve the energy conversion efficiency of the ZnO nanorod-based dye sensitized solar cells (DSSCs).

---

*Address correspondence to Prof. Sang Ho Sohn, Department of Physics, Kyungpook National University, Sangyuk-dong, Buk-gu, Daegu 702-701, Korea (ROK). Tel.: (+82)53-950-5892; Fax: (+82)53-950-6893. E-mail: shsohn@knu.ac.kr

Experimental

Synthesis

We prepared the vertically well-aligned ZnO nanorods grown on a fluorine doped tin oxide (FTO) glass using a hydrothermal method assisted with a ZnO seed layer at 90 °C for 3 hrs, then washed with ethanol, and dried at 100 °C for 1 h.

Surface modification of the ZnO nanorods was conducted by dipping in a fresh 0.1 M $TiCl_4$ solution mixed with deionized (DI) water under biasing of an ultrasonic power of 750 Watt (20 kHz) at room temperature for several minutes. Surface-modified ZnO nanorods were then washed with DI water, and dried at 70 °C for 1 h. The coating amount was adjusted by changing the dipping time. We fixed the surface modification time at 0, 10, 20, 30 and 40 min. Denomination A, B, C, D, and E implies ZnO nanorod samples prepared under surface modification time of 0, 10, 20, 30 and 40 min, respectively.

Fabrication of DSSC

DSSC devices were fabricated with a dye sensitized ZnO nanorods working electrode and a Pt-coated counter electrode, prepared by spin-coating 5 mM H_2PtCl_6 solution onto FTO and sintered at 450 °C for 30 min. Two electrodes were clipped together. They were immersed in 0.5 mmol ethanol solution of N719 dye (Dyesol) at 60 °C for 3 hrs, then washed with ethanol and dried in an oven. Two electrodes were separated by a Surlyn spacer (25 μm thick) and sealed by heating. A redox electrolyte solution (Iodolyte AN-50, Solaronix) was introduced between two electrodes.

Measurements

The comparison and analysis of the material properties between the surface-coated and the non-coated ZnO nanorods was done by the help of FE-SEM (Field Emission Scanning Electron Microscopy, HITACHI S-4800), TEM (Transmission Electron Microscopy, KJ111), XRF (X-ray Fluorescence, Philips PW2400), and UV-VIS-NIR (Ultraviolet-Visible-Near Infrared, Cary 5 spectrophotometer). I-V characteristics of ZnO nanorod-based DSSC device with the active area of 0.5×0.5 cm^2 were measured under 100 mWcm^{-2} of simulated AM 1.5 solar light by using a Solar Simulator (PEC-L12, Peccell).

Results and Discussion

Figure 1 shows the SEM images of the cross section and the top view for ZnO nanorods grown by a hydrothermal process. One can find that the hexagonal nanorods covered the entire surface of the FTO glass. Furthermore, we observed that the ZnO nanorods have the diameter of 50 or 300 nm and the length of about 2 μm, showing the preferred orientation in the c-axis direction.

Figure 2 shows TEM image of a TiO_2-coated ZnO nanorod, choosing a D sample for ease of analysis. The selected-area electron diffraction (SAED) pattern of the ZnO nanorod is shown in inset. We observed that TiO_2 shells of about 20 nm in thickness were coated on the surface of ZnO nanorods. The length and width of ZnO cores are about 2 μm and 300 nm, respectively. From the results of the SAED experiments, we observed that the ZnO nanorod has typical single-crystal nature of hexagonal ZnO, which is a crucial factor for photovoltaic device applications.

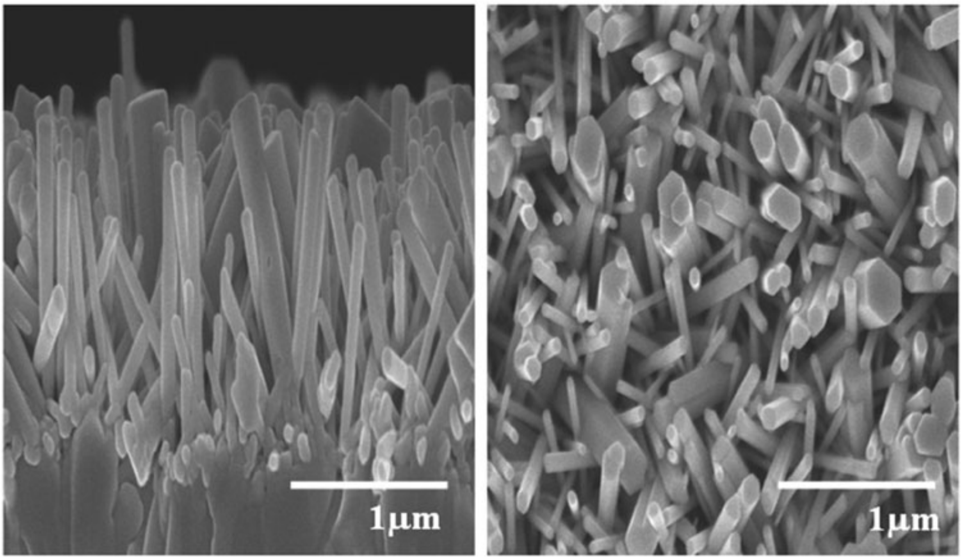

Figure 1. SEM images of the cross section and the surface for ZnO nanorods grown by a hydrothermal process.

Figure 3 shows the XRF spectra of the non-coated and TiO_2-coated ZnO nanorods, corresponding to A sample and D sample, respectively. The XRF spectra reveal that a Ti peak is observed only for the TiO_2-coated ZnO nanorod, while Zn peaks are observed in both samples. This result confirms in a roundabout way that the nano-sized oxide material coated on the surface of the ZnO nanorod is TiO_2.

Figure 4 shows the XPS spectra in the Ti 2p and O 1s region for D sample and the peak positions were referenced to carbon. Compared to TiO_2 bulk, the scan results of Ti 2p for the D sample exhibit broader peaks with a binding energy of 458.2 and 463.8 eV

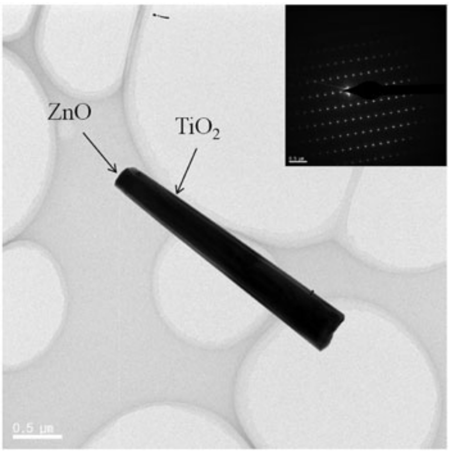

Figure 2. TEM image of a TiO_2-coated ZnO nanorod, choosing a D sample for ease of analysis. The inset figure is SAED pattern of a single ZnO nanorod. The growth direction is parallel to the c-axis.

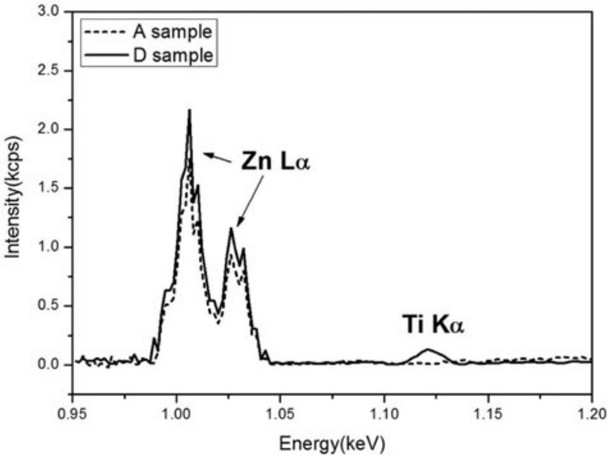

Figure 3. The XRF spectra of ZnO nanorods with and without TiO_2 modification, corresponding to D sample and A sample, respectively.

corresponding to Ti $2p_{3/2}$ and Ti $2p_{1/2}$, respectively, as shown in Fig. 4(a). The O 1s peak of the D sample was also broadened and shifted to a high binding energy, which is likely due to the mixed two peaks, corresponding to Ti-O of TiO_2 or TiOx and OH^- of Ti(OH)x, as shown in Fig. 4(b). The TiOx formation is due to the low growth temperature, and the Ti(OH)x is formed by reacting $TiCl_4$ with H_2O with assisting the sonochemical process. However, our goal is simply to form the nanolayer fast on the ZnO nanorod from $TiCl_4$ assisted sonochemical process. Therefore, Ti(OH)x and TiOx can be sufficiently applied to DSSC device, like TiO_2, to increase their photoelectrochemical properties.

Figure 5 shows the UV absorbance spectra of dyes detached from the ZnO nanorods with and without TiO_2 modifications as a function of the surface modification time in $TiCl_4$ solution under biasing of an ultrasonic power. All spectra exhibited two absorption bands at 376 and 512 nm, indicating characteristics of N719 dye [8]. To estimate the adsorbed amount of dye for five samples, we used the Beer-Lambert law. A rearranged form of the Beer-Lambert law for the ZnO nanorods allows one to calculate the number of moles of

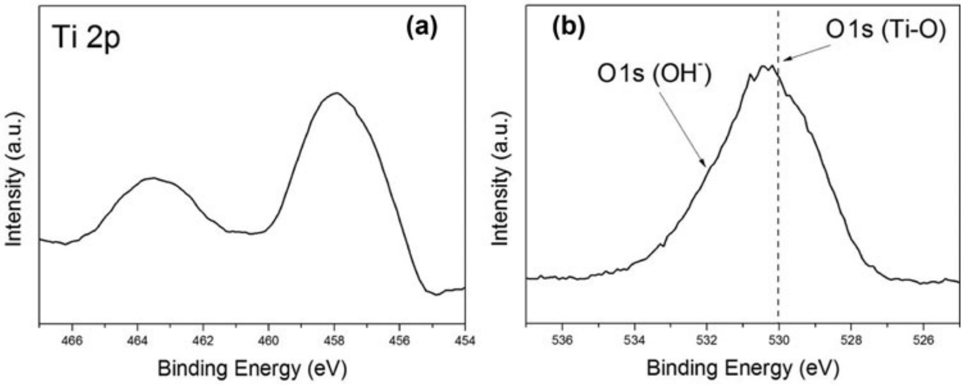

Figure 4. XPS spectra in the (a) Ti 2p and (b) O 1s region for D sample.

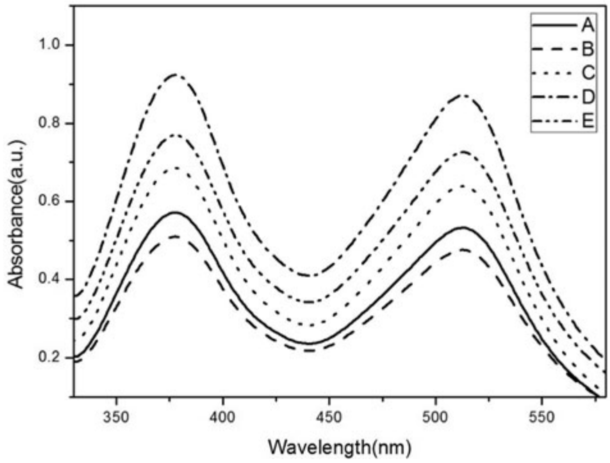

Figure 5. UV absorbance spectra of dyes detached from the ZnO nanorods with and without TiO_2 modifications.

dye adsorbed per 1 cm^2 on the surface of ZnO by the equation,

$$\alpha = \varepsilon \cdot \mathrm{l} \cdot \mathrm{c} \tag{1}$$

where α is the absorbance, ε is the molar extinction coefficient of the dye in solution ($M^{-1}\cdot cm^{-1}$), l is the path length (cm) and c is the concentration of the sample solution (M). UV-Vis absorption spectra of the resultant solution, whose molar extinction coefficient was determined to be 1.41×10^4 dm^3 mol^{-1} cm^{-1} at 515 nm [9], were measured using a 1 cm quartz cell to estimate the adsorbed amount of dye. Using the given values, $\varepsilon = 1.41 \times 10^4$ dm^3 mol^{-1} cm^{-1} at 515 nm, l = 1 cm, and the α values measured at 515 nm, we can calculate the concentration c by equation (1). The physical characteristics of ZnO nanorods obtained in this way are listed in Table 1. The spectra and calculated concentrations tell that the absorbance increases in the order of B, A, C, E, and D samples due to the surface treatment effects as a function of surface treatment time, implying the thickness effects of TiO_2 shells. However, the B sample has poor absorbance, compared to A sample, which is likely due to the amorphous phase of the TiO_2 shell with thin thickness. Furthermore, the

Table 1. Physical characteristics of the ZnO nanorods vs surface modification time

Samples	Surface modification time	Absorbance at 515 nm	Adsorbed N719[a] ($mol\cdot dm^{-3}$)
A	0 min	0.53	3.76×10^{-6}
B	10 min	0.47	3.33×10^{-6}
C	20 min	0.64	4.54×10^{-6}
D	30 min	0.87	6.17×10^{-6}
E	40 min	0.72	5.11×10^{-6}

[a] Amounts of adsorbed N719 were calculated from the UV-Vis absorption spectra by using Beer-Lambert's law.

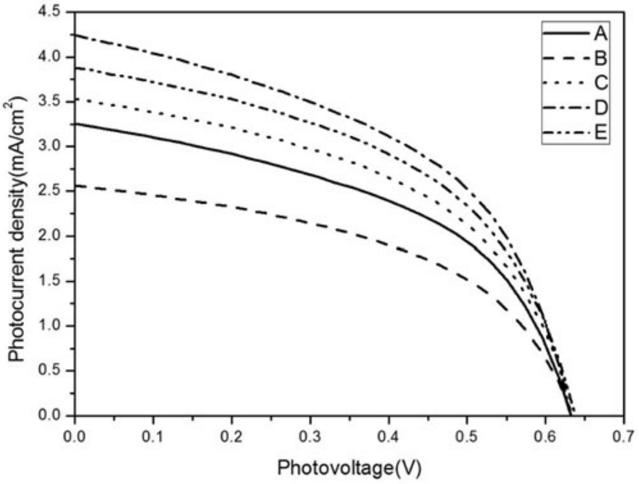

Figure 6. I-V curves of DSSCs fabricated by using ZnO nanorods with and without TiO_2 modification from $TiCl_4$ assisted sonochemical process.

absorbance of E sample reduced more than that of D sample, which is probably because of thick thickness of the TiO_2 shell, leading to a reduced surface area.

Figure 6 shows the photocurrent density (I) vs. photovoltage (V) curves of the DSSCs fabricated by using ZnO nanorods with and without TiO_2 modification from a $TiCl_4$ assisted sonochemical process. The electro-optical characteristics of DSSCs are also listed in Table 2. One can find that there was no significant difference in V_{OC} between non- and TiO_2-coated ZnO nanorods-based DSSCs. With increasing TiO_2 surface treatment time of the ZnO nanorods, the energy conversion efficiencies gradually increase, except for E device. A maximum efficiency of 1.37% was achieved in case of D device with short-circuit current density (J_{SC}) = 4.25 mA·cm^{-2}, open-circuit voltage (V_{OC}) = 635.8 mV and fill factor (FF) = 50.7% as listed in Table 2. The enhancement of the energy conversion efficiency originates from the increased J_{SC} and V_{OC} in the DSSC devices with ZnO nanorods that are suitably coated TiO_2 shell. These facts can be explained as follows. The TiO_2 nanolayer can form new energy barrier on the ZnO nanorods, which can effectively inhibit the surface charge recombination and improve the energy conversion efficiency of the ZnO nanorod-based dye sensitized solar cells (DSSCs).

Table 2. Electro-optical characteristics of DSSCs with ZnO nanorods

DSSC devices	V_{oc} (mV)	J_{sc} (mA/cm^2)	FF (%)	Efficiency (%)
A	635.3	3.30	50.2	1.05
B	634.4	2.57	50.2	0.82
C	635.7	3.55	50.8	1.15
D	635.8	4.25	50.7	1.37
E	635.5	3.87	50.6	1.24

The complex trend in efficiencies can be explained as follows. TiO_2 nanolayer formed by dipping in less than 10min is probably amorphous and remains the dye aggregates in sensitization process, which causes poor electron injection, slow diffusion, and low J_{SC} values. TiO_2 nanolayers were formed by dipping for 10 – 30 min, and J_{SC} value consistently increases due to gradual crystallization of the nanolayers. On the other hand, DSSCs with TiO_2 nanolayer formed by dipping for 40 min reveal a slight decrease in J_{SC} due to a reduced surface area, leading to smaller dye loading. Therefore, we conclude that DSSCs with TiO_2 nanolayer formed by dipping for 30 min exhibits best efficiencies

Conclusions

The ZnO nanorods with the diameter of 50 and 300 nm and the length of 2 μm are grown on the FTO glass with a ZnO seed layer by the hydrothermal process, which display the preferred orientation in the c-axis direction. Surface modification on the ZnO nanorods by TiO_2 was carried out by the sonolysis of $TiCl_4$, changing modification time. The results demonstrate that an TiO_2 nanolayer can effectively inhibit the surface charge recombination and improve the energy conversion efficiency of the ZnO nanorod-based dye sensitized solar cells (DSSCs). The highest conversion efficiency obtained was 1.37% for the dye-sensitized ZnO nanorods with $TiCl_4$ modification time of 30 min during the sonochemical process.

Acknowledgment

This research was supported by Basic Science Research Program through the National Research Foundation of Korea (NRF) funded by the Ministry of Education, Science and Technology (2013R1A1A4A01008503).

References

[1] O'Regan, B., & Gratzel, M. (1991). *Nature*, *353*, 737.

[2] Gratzel, M. (2005). *Inorg. Chem.*, *44*, 6841.

[3] Keis, K., Magnusson, E., Lindstrom, H., Lindquist, S. E., & Hagfeldt, A. (2002). *Sol. Energy Mater. Sol. Cells*, *73*, 51.

[4] Law, M., Greene, L. E., Johnson, J. C., Saykally, R., & Yang, P. (2005). *Nat. Mater.*, *4*, 455.

[5] Ko, S. H., Lee, D. H., Kang, H. W., Nam, K. H., Yeo, J. Y., Hong, S. J., Grigoropoulos, C. P., & Sung, H. J. (2011). *Nano Lett.*, *11*, 666.

[6] Lu, L., Li, R., Peng, T., Fan, K., & Dai, K. (2011). *Renewable Energy*, *36*, 3386.

[7] Ueno, S., & Fujihara, S. (2011). *Electrochim. Acta*, *56*, 2906.

[8] Nazeeruddin, M. K., Kay, A., Rodicio, I., Humphry-Baker, R., Muller, E., Liska, P., Vlachopoulos, N., & Gratzel, M. (1993). *J. Am. Chem. Soc. 115*, 6382.

[9] Wang, Z. S., Kawauchi, H., Kashima, T., & Arakawa, H. (2004). *Coord. Chem. Rev. 248*, 1381.